scientific reports

Check for updates

OPEN

Repurposing SARS CoV 2 ligands identifies salvianolic acid C as potential antiviral candidate against human metapneumovirus through computational study

Pallavi Mosale Shanthappa[1]✉, Nidheesh Melethadathil[2] & Shiva Prasad Kollur[3]

Human Metapneumovirus (HMPV) is a leading cause of respiratory tract infections worldwide, with no approved antiviral treatments or vaccines currently available. This study explores the potential of repurposing SARS-CoV-2 ligands as therapeutic agents against HMPV through a comprehensive computational approach. The present study investigates three ligands, Salvianolic Acid C, Mycophenolic Acid, and Aurintricarboxylic Acid for their binding affinity, stability, and interaction dynamics with the HMPV protein structure using molecular docking, molecular dynamics (MD) simulations, binding free energy calculations, and principal component analysis (PCA). The results revealed that Salvianolic Acid C formed the most stable complex with HMPV protein model, exhibiting consistent RMSD values (5–6 Å), low residual fluctuations, and a favorable binding free energy of -26.12 kcal/mol. Hydrogen bond analysis further supported its stability, with a 20.97% occupancy between GLU96 of HMPV protein model and Salvianolic Acid C. In contrast, Mycophenolic Acid and Aurintricarboxylic Acid demonstrated weaker binding and higher conformational heterogeneity. PCA and free energy landscape (FEL) analysis confirmed the stable binding mode of Salvianolic Acid C, with well-defined, deep energy basins, while the other ligands exhibited fragmented and less stable conformations. Furthermore, these findings highlight that Salvianolic Acid C as a promising candidate for anti-HMPV therapy, leveraging its stable binding and favorable thermodynamic properties. This study provides a foundation for the development of targeted antiviral treatments against HMPV protein model, addressing a critical unmet need in respiratory disease management for further experimental validation.

Keywords Human metapneumovirus, HMPV, SARS-CoV-2, Drug repurposing, Salvianolic acid C, Molecular docking and dynamics, Antiviral therapy

Human metapneumovirus (HMPV) has been recognized as a significant cause of respiratory tract illness in both children and adults worldwide[1]. First identified in 2001[2], HMPV can cause a wide range of respiratory illnesses, from mild upper respiratory tract infections (URTIs) to severe lower respiratory tract infections (LRTIs) such as bronchiolitis and pneumonia[2,3]. HMPV belongs to the family *Paramyxoviridae*, genus *Metapneumovirus*[2,4]. Its genome consists of a single-stranded, negative-sense RNA molecule[2,5]. The virus has two major genetic lineages, A and B, which are further subdivided into multiple subtypes[6–8]. These subtypes exhibit genetic variations that may influence infection severity[6,7].

Symptoms of HMPV infection may include cough, congestion, fever, and, in severe cases, respiratory failure requiring hospitalization[9]. The protein structure of HMPV is characterized primarily by its fusion (F) glycoprotein, which plays a crucial role in viral entry into host cells. The F protein exists in two main conformations: prefusion and postfusion[10]. HMPV primarily infects ciliated epithelial cells in the respiratory tract[11]. Initial binding and infection are mediated by interactions between the viral F protein and heparan sulfate

[1]Department of Computer Science, School of Computing, Amrita Vishwa Vidyapeetham, Mysuru Campus, India. [2]School of Biotechnology, Amrita Vishwa Vidyapeetham, Amritapuri Campus, Kollam, India. [3]School of Physical Sciences, Amrita Vishwa Vidyapeetham, Mysuru Campus, Mysuru 570 026, Karnataka, India. ✉email: ms_pallavi@my.amrita.edu

(HS) on the host cell surface[12]. The F protein is essential for viral entry and membrane fusion[12,13]. Once inside the host cell, the virus replicates within the cytoplasm, forming inclusion bodies (IBs)[5,14]. These IBs are dynamic, liquid-like structures that facilitate efficient viral replication and transcription[5]. The viral phosphoprotein (P) plays a key role in IB formation, independently driving phase separation and recruiting the nucleoprotein (N)[5]. Interestingly, HMPV spreads between cells through both virion budding and direct cell-to-cell transmission via intercellular extensions[14]. These extensions facilitate the transfer of inclusion bodies, representing a novel mechanism of direct viral spread[9,14].

Despite its significant impact, there remains a critical need for effective treatments and vaccines against HMPV[3,11,15]. Currently, there are no licensed antiviral drugs or vaccines specifically targeting HMPV[2,3,15]. Treatment primarily focuses on supportive care, including oxygen therapy, fluid management, and symptomatic relief[16,17]. In severe cases, mechanical ventilation may be required[18]. Given the absence of targeted therapies, drug repurposing strategies are being explored to identify existing drugs with potential anti-HMPV activity[15]. Several compounds, such as mycophenolic acid and aurintricarboxylic acid, have demonstrated inhibitory effects against HMPV replication[15].

This study explores the potential repurposing of SARS-CoV-2 (Severe Acute Respiratory Syndrome Coronavirus 2) ligands for HMPV protein model, as both viruses cause respiratory tract infections. Initially, a SARS-CoV-2 strain was selected, and available ligands for that strain were identified. The ligands were then filtered based on ADME (Absorption, Distribution, Metabolism, and Excretion) properties to exclude unsuitable structures. The top-selected ligand, Salvianolic Acid C, is a water-soluble phenolic compound primarily derived from the roots of *Salvia miltiorrhiza* (commonly known as Danshen), a traditional Chinese medicinal herb[19,20]. Salvianolic Acid C belongs to the class of depsides, consisting of caffeic acid derivatives, and is known for its potent antioxidant and anti-inflammatory properties. The docking of Salvianolic Acid C with the HMPV protein structure was followed by molecular dynamics simulation, binding free energy estimation, and PCA (Principal Component Analysis).

Mycophenolic acid, a potent immunosuppressant agent that inhibits purine biosynthesis, was originally derived from *Penicillium stoloniferum*. It has also exhibited antibacterial, antifungal, and antiviral properties[21]. Aurintricarboxylic acid, a versatile compound with applications in molecular biology, virology, and cancer research, has shown the ability to inhibit critical cellular processes. This makes it a valuable tool in scientific studies aimed at understanding complex biological interactions and developing novel therapeutic strategies[22]. These findings provide promising leads for the development of antiviral therapies against HMPV.

Materials and methodologies

Retrieval of protein structure for HMPV and ligands

The UniProt ID "Q91KZ5" was used to retrieve the number of HMPV protein structures available to date, along with their PDB ID details. The ligands used in this study were extracted based on active ligand components targeting SARS-CoV-2. Initially, the UniProt ID "P59594," corresponding to SARS-CoV-2, was used to extract the active ligands. These ligands were then filtered based on ADME properties and to exclude unwanted structures.

Ligand preparation and optimization

All the ligands listed in Table 1 were retrieved from PubChem[23] in the sdf file format. The PDB file for these sdf files was obtained from online web tool cheminfo through OpenBabel[24]. The structures' geometry was cleaned and examined using Chimera[25]. The 3-dimensional geometries of the selected ligands were optimized by ORCA tool[26]. The input to ORCA tool was generated using AVOGRDO2[27] visualization and optimized via ORCA. The B3LYP method was chosen for the optimization and frequency calculations. The B3LYP functional method provides an excellent compromise between accuracy and computation[28]. Frontier molecular orbitals, i.e., HOMO (Highest Occupied Molecular Orbital) and LOMO (Lowest Unoccupied Molecular Orbital) orbitals, for the compounds were calculated using the same level of theory. The ligand optimization was successfully applied in various previous computational studies[29] and advances in development of antivirals for respiratory viruses[30].

Binding site prediction and performing molecular docking

The binding site for the HMPV protein model was predicted using the CASTp (Computed Atlas of Surface Topography of proteins)[31] tool. The ligand PDB files were cleaned using "pdb_uniqname.py" before it was uploaded to HADDOCK 2.4 web tool[32] to perform molecular docking.

Molecular interactions

The ligands and the HMPV protein complex, which expressed high binding affinity with the least binding energy, were analyzed for molecular interaction studies through LigPlot+[33] tool. This tool is employed to create 2D diagrams of ligand-protein interactions using 3D coordinates, offering precise information about molecular interactions and Chimera.

Molecular dynamics

The ligand-HMPV protein complex with the lowest binding energy was considered for molecular dynamics simulation. GROMACS employs the Velocity Verlet al.gorithm to numerically integrate Newton's equations of motion during the simulation, hence ensuring precise trajectory calculations. The simulations were conducted using the NVE ensemble, which ensured that the number of particles, volume, and energy remained constant throughout the whole simulation. The GROMACS 2024.2[34] was applied with an Amber ff99SB-ILDN force field[35]. The topology parameters for HMPV protein model were created using the Gromacs program, and the topology parameters of ligands were built using the antechamber using the AMBER22 suite[36,37]. The complex was immersed in a dodecahedron box with extended simple point charge water molecules[38]. By adding ions,

Ligand Name and molecular formula and weight	Smiles	RoMol 3D structure
Salvianolic acid C (SAC) $C_{36}H_{20}O_{10}$ 492.4 g/mol	*C1 = CC(= C(C = C1C[C@H](C(= O)O)OC (= O)/C = C/C2 = C3C = C(OC3 = C(C = C2) O)C4 = CC(= C(C = C4)O)O)O)O*	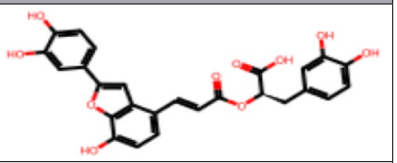
Mycophenolic acid (MPA) $C_{17}H_{20}O_6$	*CC1 = C2COC(= O)C2 = C(C(= C1OC)C /C = C(\C)/CCC(= O)O)O*	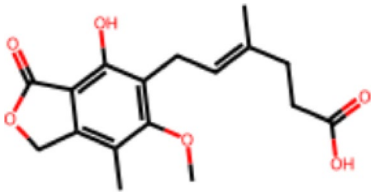
Aurintricarboxylic acid (ATA) $C_{22}H_{14}O_9$	*C1 = CC(= C(C = C1C(= C2C = CC(= O)C(= C2)C(= O)O)C3 = CC(= C(C = C3)O) C(= O)O)C(= O)O)O*	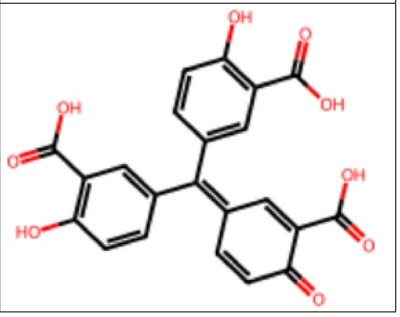

Table 1. Candidate ligand and drug information used in this study.

the system was neutralized. The steepest descent minimization approach reduces energy consumption (50,000 steps). The system gets heated to 300 K during the 1000 ps NVT scenario. The 1000 ps NPT simulation equalizes the pressure to 1 atm. The MD simulation was performed for 200 ns to analyze the conformational stability of the complex. The Root Mean Square Fluctuation (RMSF) and Root Mean Square Deviation (RMSD) were extracted from the trajectory to analyze the stability of the complexes. The plots were made using Xmgrace software[39].

Binding free energy calculations

To further verify the binding stability of the complexes, binding free energy is calculated with the help of the GMXPBSA MMPBSA.py[40] module. The output files of MD simulations like the tpr file, index, trajectory, and topology file are used as the input for the module; these files are used to create AMBER topology. The mmpbsa. in file contains the MMPBSA calculation specifications, which are used to calculate binding free energy.

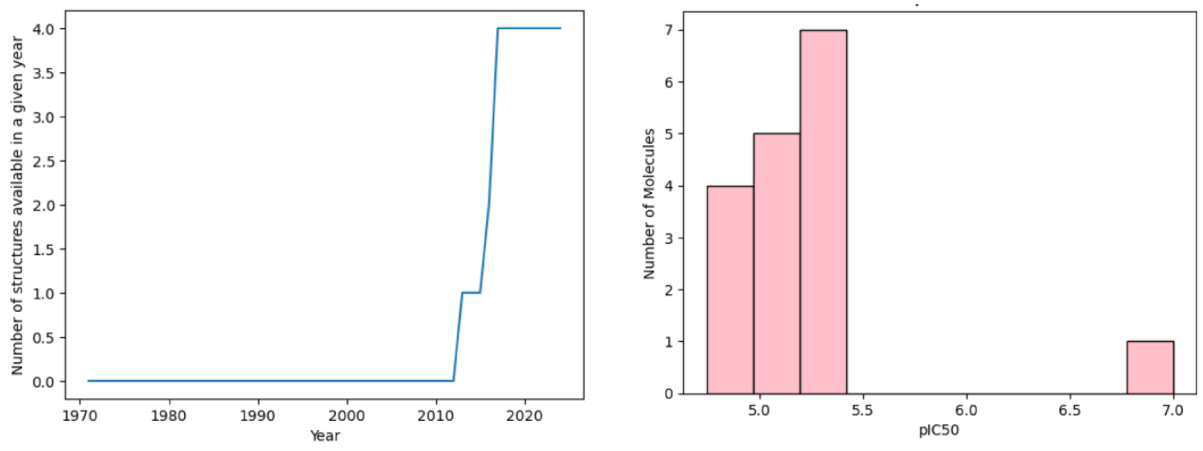

Fig. 1. (**a**) Retrieved of protein structures the UniProt ID "Q91KZ5" against HMPV protein model (**b**) Ligand components from the RCSB with pIC50 values between four and seven.

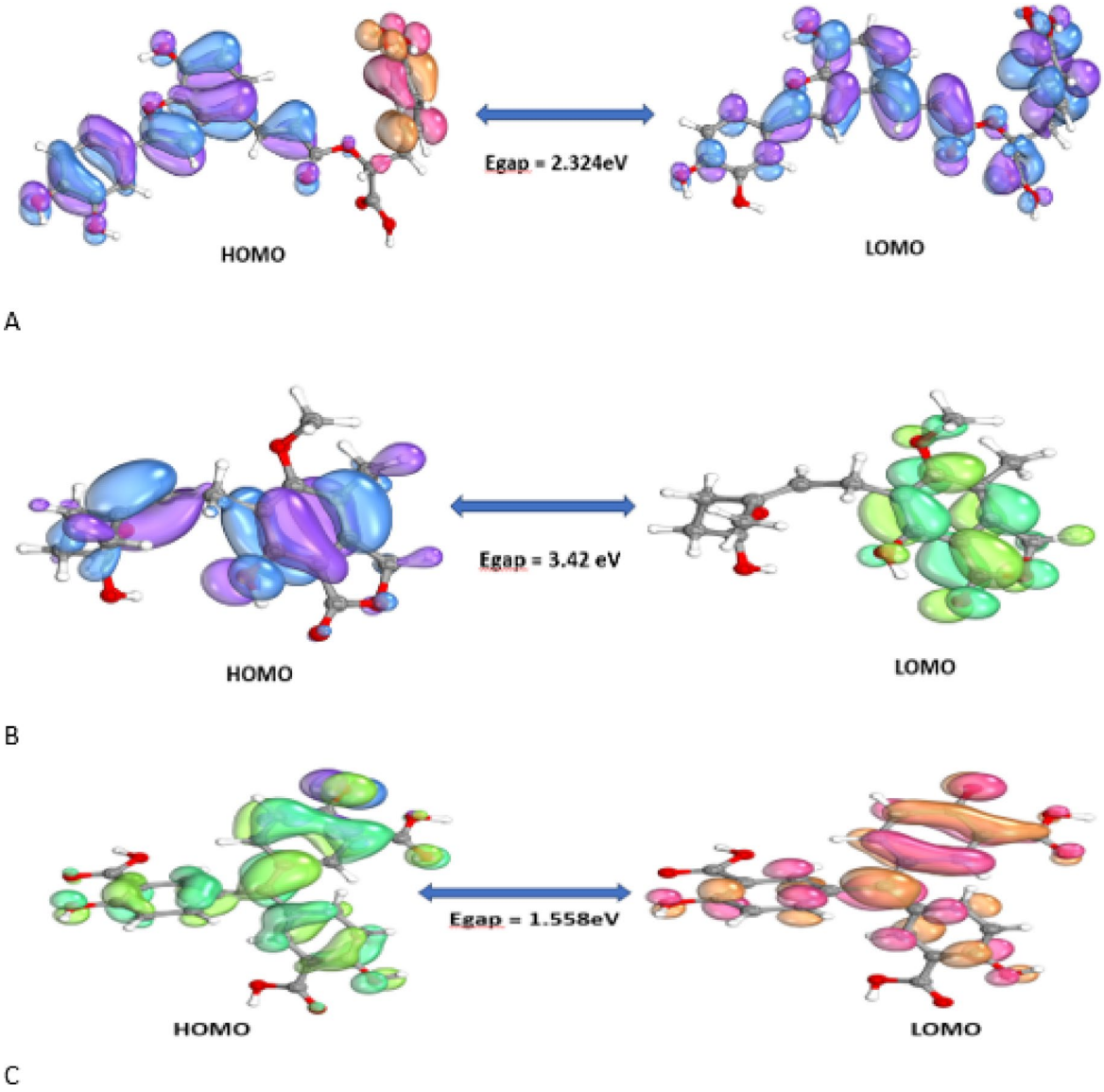

Fig. 2. Optimization of ligands using DFT geometry optimization technique (**A**) Salvianolic acid C, (**B**) Mycophenolic acid, and (**C**) Aurintricarboxylic acid.

Principal component analysis (PCA) and free energy landscape (FEL) analysis

PCA was used to analyze trajectory's high amplitude concerted motion leveraging the eigenvectors derived from the mass-weighted covariance matrix of protein atomic fluctuations. The cosine content (ci) of each principal component (pi) in the covariance matrix was computed to construct the free energy landscape via PCA analysis. GROMACS's built-in tools, "g_covar" for generating the covariance matrix with the protein backbone as a reference structure for rotational fitting, and "g_anaeig" for analyzing and visualizing the eigenvectors, were employed. Principal components exhibiting smaller cosine content values, typically below 0.2, tend to produce qualitatively superior results, often showing a single basin[41]. The Free Energy Landscape (FEL) was constructed by utilizing the cosine contents of the first two projection eigenvectors (referred to as PC1 and PC2) that were below 0.2. The methodologies applied in this study are successfully applied in various previous computational studies[42–47].

Results

Retrieval of protein structure for HMPV and ligands

A total of four protein structures were retrieved for the UniProt ID "Q91KZ5" against HMPV; these protein structures were deposited in the RCSB Protein Data Bank after the year 2011 as shown in Fig. 1a. To obtain the protein structure, the experimental method used was "X-RAY DIFFRACTION," with a maximum resolution of 4.0 Å, four chains, and a minimum ligand molecular weight of 10.0 g per mole. Based on this query, the selected PDB ID was "5WB0," which was retrieved with a resolution of 1.86 Å.

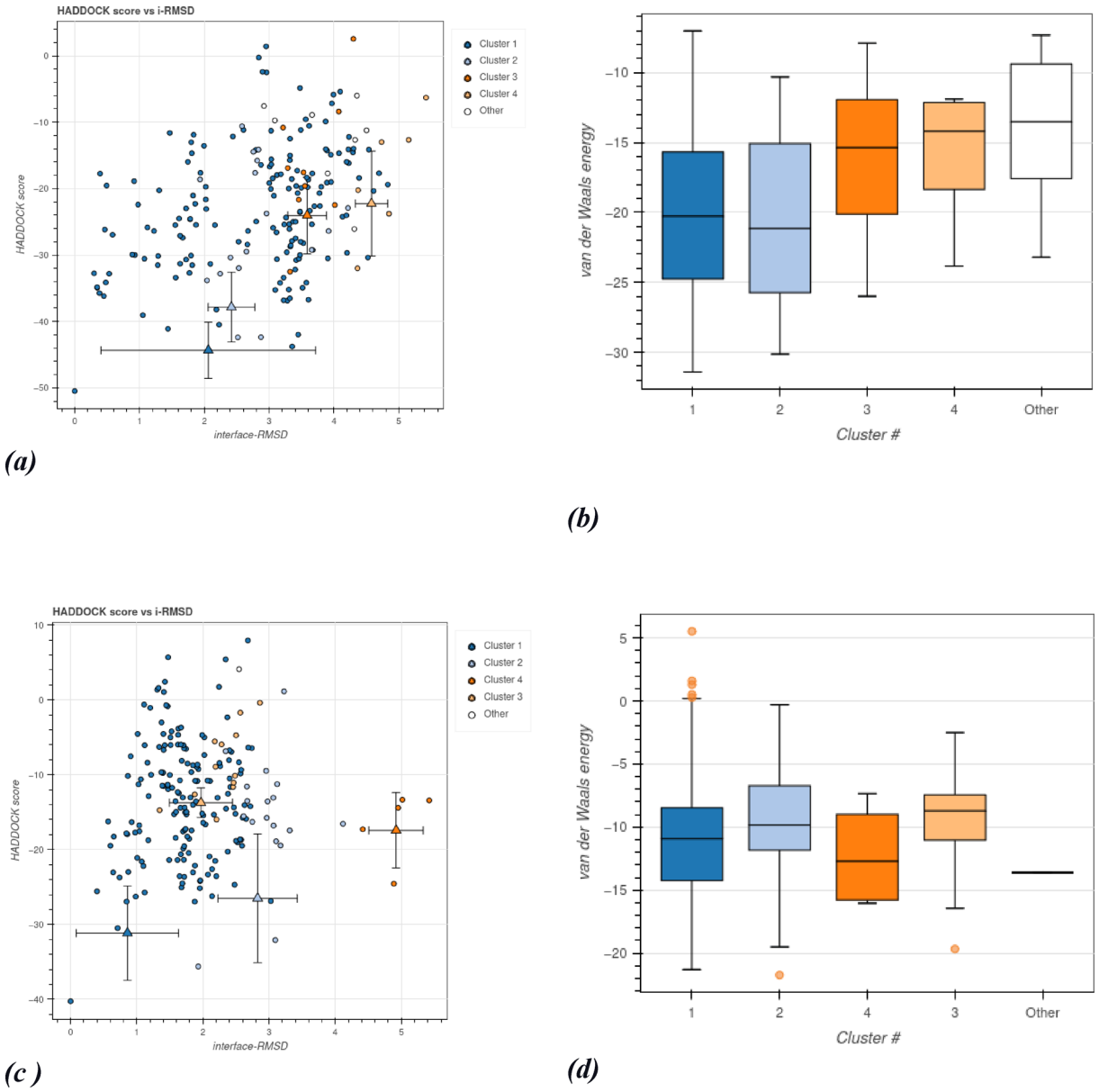

Fig. 3. (**a**) Model Analysis Salvianolic acid C with HMPV protein complex, (**b**) Cluster Analysis of Salvianolic acid C with HMPV protein complex, (**c**) Model Analysis Mycophenolic acid with HMPV protein complex, (**d**) Cluster Analysis of Mycophenolic acid with HMPV protein complex, (**e**) Model Analysis Aurintricarboxylic acid with HMPV protein complex, and (**f**) Cluster Analysis of Aurintricarboxylic acid with HMPV protein complex.

The target organism "Severe Acute Respiratory Syndrome Coronavirus" with Spike glycoprotein as the preferred target was selected. All ligands bioactive against the Spike glycoprotein were listed and subsequently filtered for unwanted substructures and ADMET properties. Further, ligand-based screening was performed using Lipinski's Rule of Five against the target protein structure of Human Metapneumovirus (HMPV) to select the ligands. Considering two protein structures for SARS-CoV2, a total of 17 ligand components were retrieved from the RCSB Protein Data Bank, which had pIC50 values between four and seven, as shown in Fig. 1b. These ligands were then filtered based on ADME properties and to exclude unwanted structures, finally selecting three active ligand candidates.

The selected ligand/drug candidates for this study, along with their respective chemical 3D structures, molecular formula, and molecular weight, are listed in Table 1. This table provides a comprehensive overview of the compounds under study, highlighting their key properties and relevance to the study's objectives. The results of HOMO (Highest Occupied Molecular Orbital) and LOMO (Lowest Unoccupied Molecular Orbital) and energy gap are shown in Fig. 2, an energy gap of 1.558 eV (Aurintricarboxylic acid (Fig. 2C)) indicates a low gap, suggesting that the molecule is highly reactive and may easily participate in electron transfer processes. While this may enhance its biological activity, it could also imply lower chemical stability, which may pose challenges

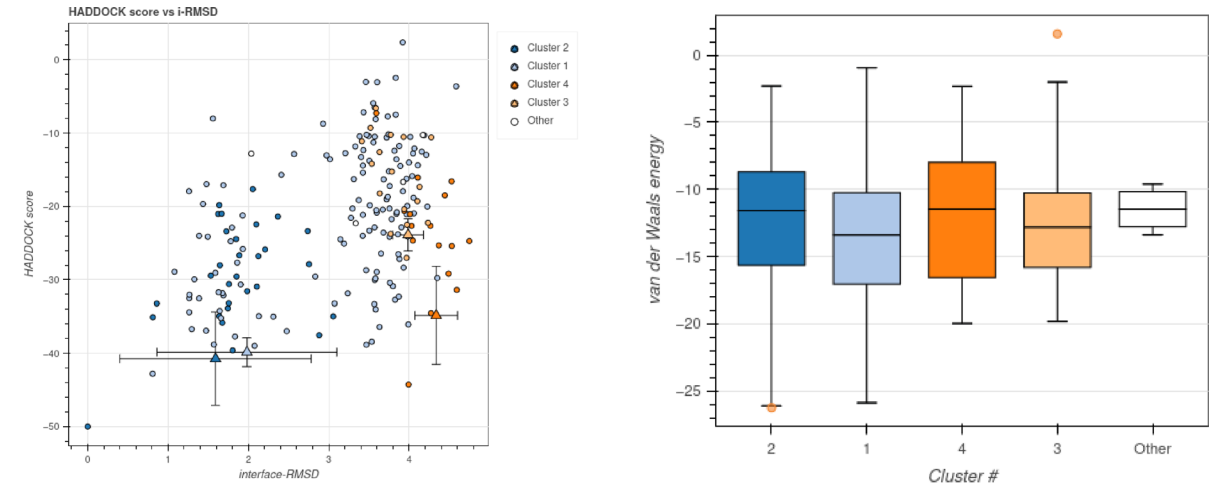

(e) *(f)*

Fig. 3. (continued)

related to toxicity or degradation. An energy gap of 2.324 eV (Salvianolic acid C (Fig. 2A)) is considered moderate. Molecules with this gap tend to offer a good balance between reactivity and stability, making them potentially suitable for bioactive applications. This range often aligns well with drug-likeness, where the molecule is reactive enough to interact with biological targets but still stable enough for therapeutic use. In contrast, an energy gap of 3.42 eV (Mycophenolic acid (Fig. 2B)) is relatively high, indicating a more stable but less reactive molecule.

Molecular docking analysis

Analysis of salvianolic acid C (SAC) with HMPV(5WB0)

The molecular docking analysis provides critical insights into the binding interactions of three repurposed ligands Salvianolic Acid C, Mycophenolic Acid, and Aurintricarboxylic Acid with the Human Metapneumovirus (HMPV) protein (PDB: 5WB0). Binding energy of SAC HADOCK Score (−44.3 +/- 3.7), Binding energy of MPA HADDOCK Score (−31.2 +/- 5.5) and Binding energy of ATA HADOCK Score (−40.7 +/- 5.5).

The results are visualized in Fig. 3, which includes model analyses (a, c, e) and cluster analyses (b, d, f) for each ligand.

Salvianolic acid C (Fig. 3a,b)

The Model Analysis (3a) of Salvianolic Acid C exhibits a strong binding pose within the active site of HMPV protein model, forming multiple hydrogen bonds and hydrophobic interactions. The ligand fits snugly into the binding pocket, suggesting low steric clashes and high complementarity with the viral protein. Cluster Analysis (3b) reveals a dominant binding conformation, with a high population density in the most stable pose. This indicates low conformational flexibility and reinforces the ligand's stability when bound to HMPV protein model.

Mycophenolic acid (MPA) (Fig. 3c,d)

The Model Analysis (3c) of Mycophenolic Acid binds to HMPV protein model but with fewer hydrogen bonds compared to Salvianolic Acid C. The binding site shows moderate affinity, with some polar interactions but weaker hydrophobic stabilization. Cluster Analysis (3d) distribution is less concentrated, indicating higher conformational heterogeneity. Multiple suboptimal poses suggest lower binding stability compared to Salvianolic Acid C.

Aurintricarboxylic acid (ATA) (Fig. 3e,f)

The Model Analysis (3e) of Aurintricarboxylic Acid shows bulky binding, leading to potential steric hindrance within the HMPV protein active site. Despite some ionic/polar interactions, the ligand's large size may disrupt optimal binding. Cluster Analysis (3f) are widely dispersed, reflecting poor convergence to a single stable conformation. This suggests high flexibility and weak binding stability.

Thus, Salvianolic Acid C emerges as the top candidate due to its strong, stable, and well-defined interactions with the HMPV protein model used in this study. Mycophenolic Acid and Aurintricarboxylic Acid exhibit weaker binding and higher conformational variability, diminishing their therapeutic potential.

Binding interaction analysis

The salvianolic acid C with HMPV(5WB0) complex

The salvianolic acid C with HMPV(5WB0) complex forms multiple hydrogen bonds with Arg101(A), Val112(A), Lys324(A), and Glu327(A), with distances between 2.39 Å and 3.29 Å. These interactions involve both polar and

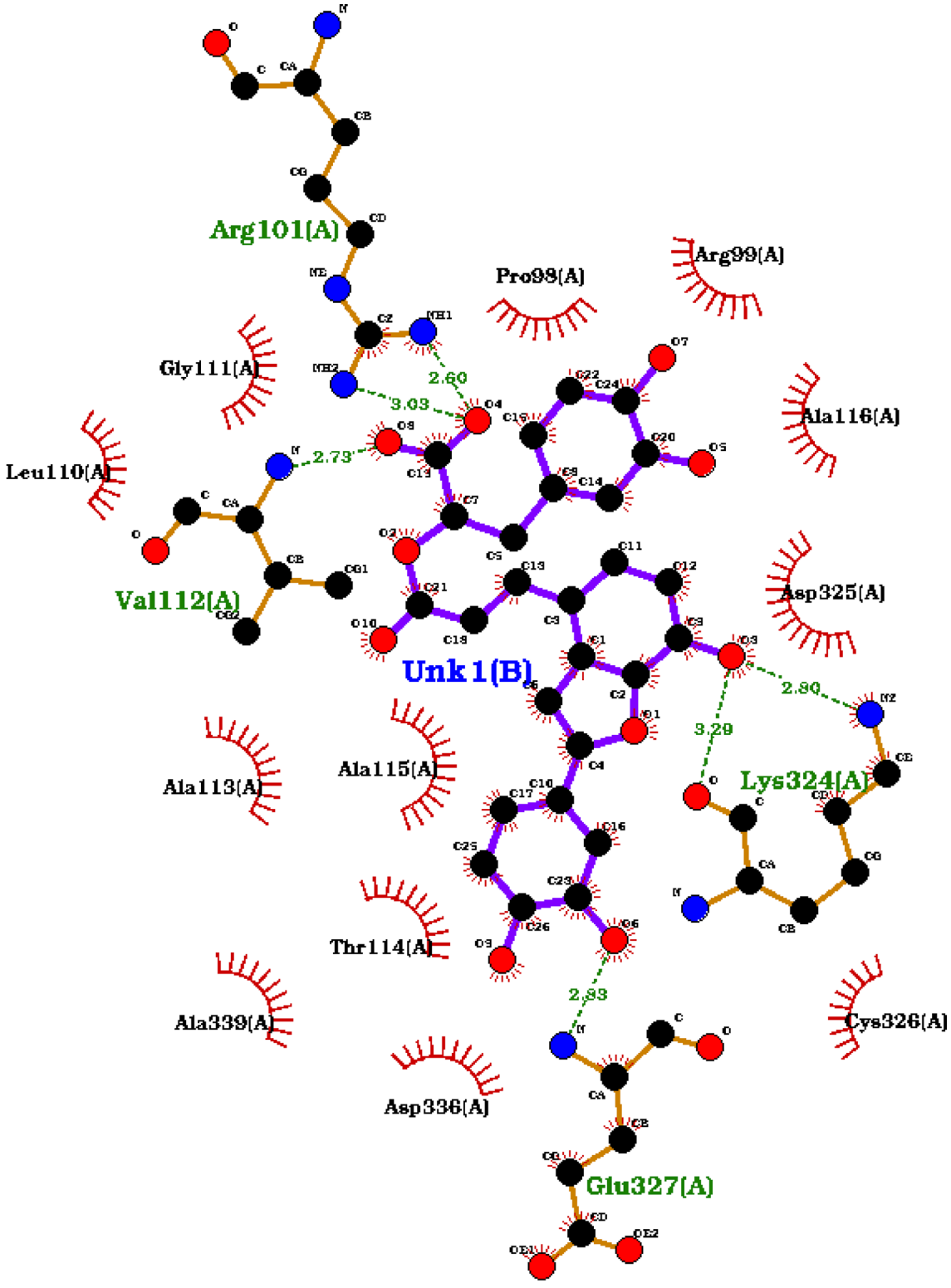

(a)

Fig. 4. Molecular interaction results (**a**) salvianolic acid C with HMPV(5WB0) complex, (**b**) Mycophenolic acid with HMPV(5WB0) complex, and (**c**) Aurintricarboxylic acid with HMPV(5WB0) complex (the green dotted lines indicate hydrogen bonds and red residues with electrostatic interactions).

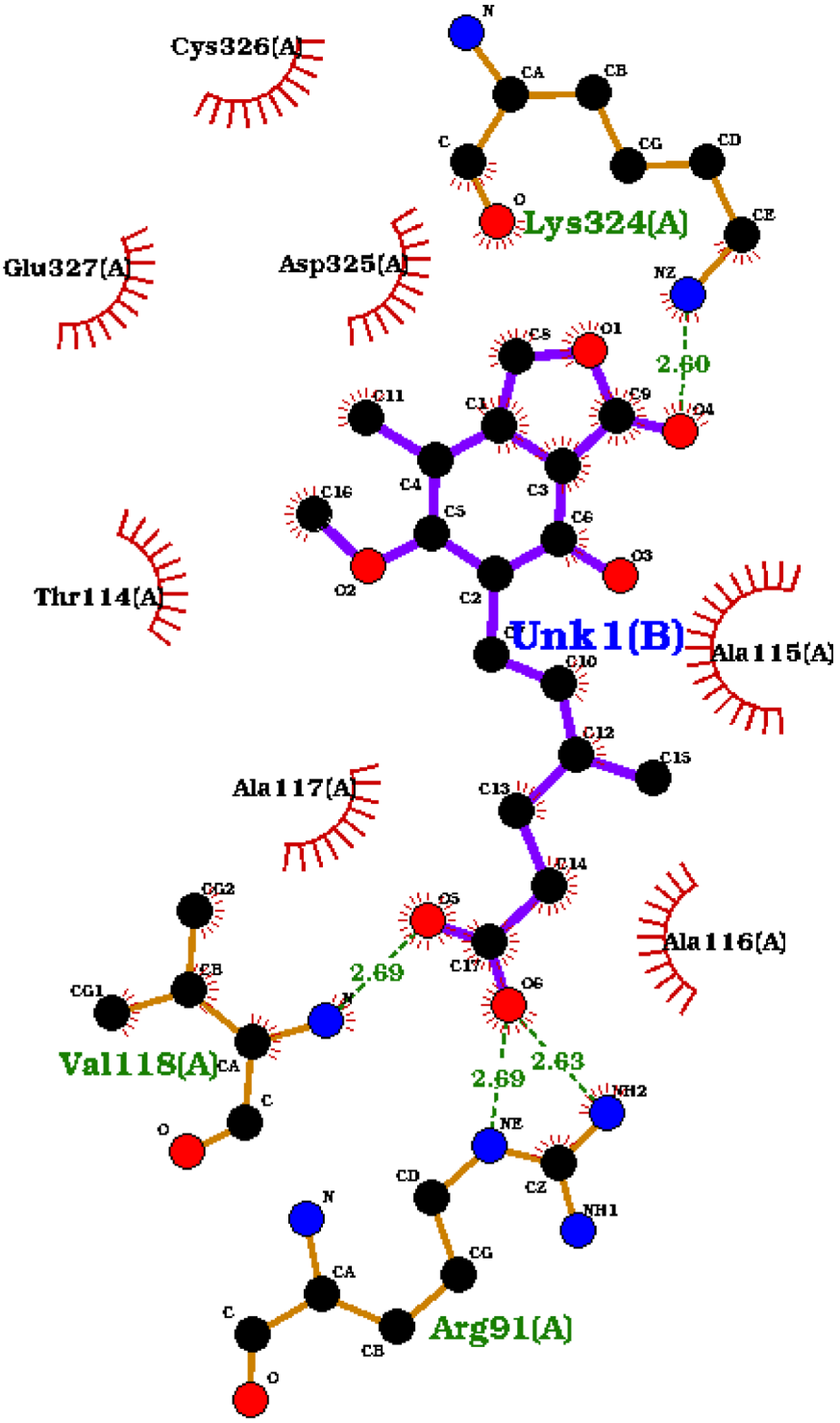

(b)

Fig. 4. (continued)

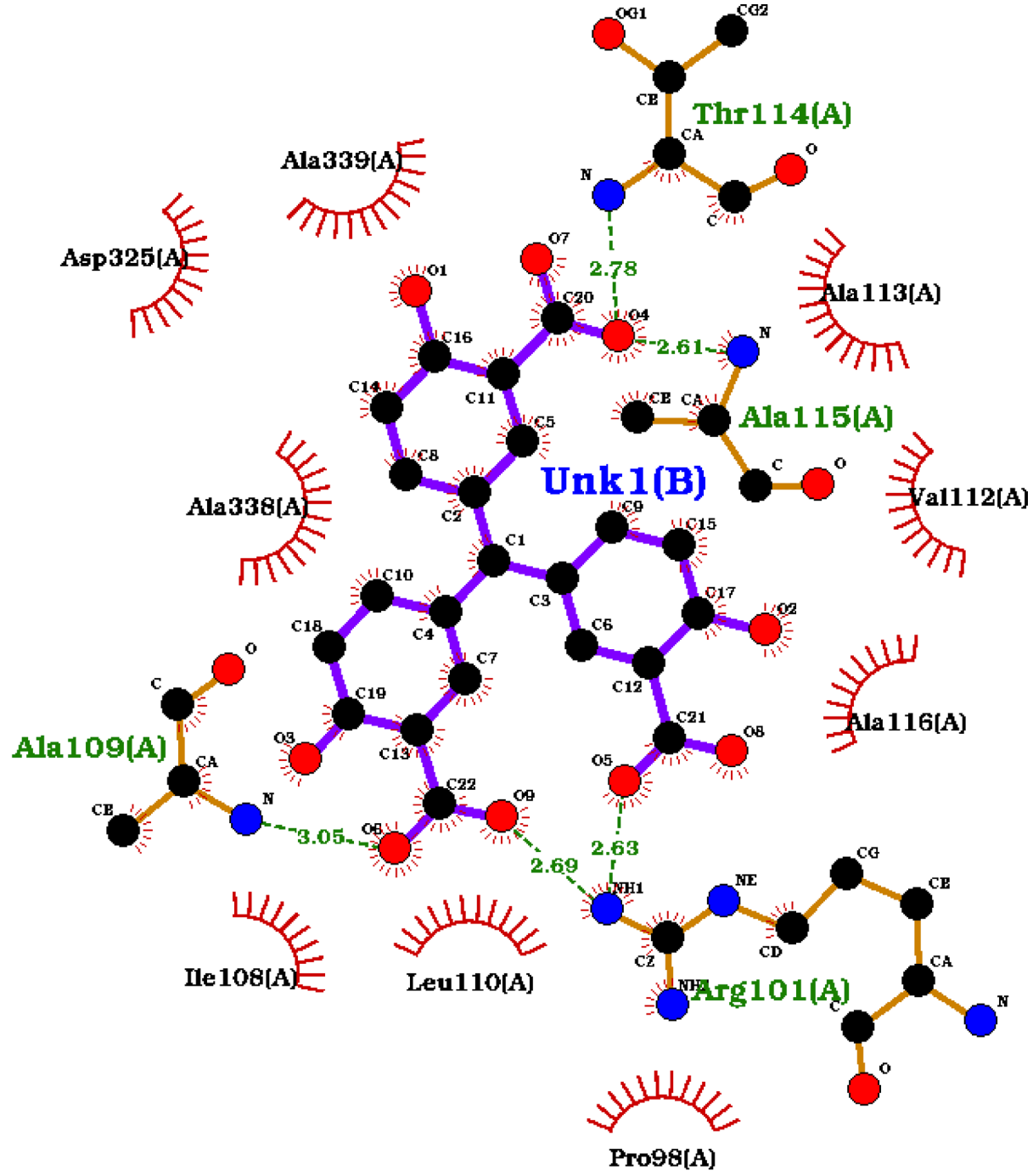

(c)

Fig. 4. (continued)

charged residues, providing strong stabilization of the ligand. Alongside these, hydrophobic interactions with residues such as Leu110, Pro98, Gly111, Ala113, Ala115, Ala116, Asp325, Ala338, and Ala339 create a robust binding environment. The combination of multiple hydrogen bonds and widespread hydrophobic contacts indicates that this ligand likely binds more strongly and stably than in the other two cases, as illustrated in Fig. 4a and detailed in Table 2.

Molecular interactions		
Complex	**HMPV (5WB0)**	**Hydrogen bond distance in Å**
The salvianolic acid C with HMPV (5WB0) protein complex	ARG101 VAL112 LYS324 GLU327	2.60 2.73 2.80 2.83
The mycophenolic acid with HMPV (5WB0) Complex	ARG91 VAL118 LYS324	2.63 2.69 2.60
The aurintricarboxylic acid with HMPV (5WB0) Complex	ARG101 ALA109 THR114 ALA115	2.63 3.05 2.78 2.61

Table 2. Molecular interactions with HMPV protein model (A) and ligand (B) with H-bonds distance in Å.

The mycophenolic acid with HMPV(5WB0) complex

The mycophenolic acid with HMPV(5WB0) shows a network of stabilizing interactions, with strong hydrogen bonding to Lys324(A), Val118(A), and Arg91(A), with bond lengths between 2.68 Å and 2.90 Å. The involvement of positively charged residues like Lys324 and Arg91 indicates electrostatic contributions that enhance ligand stability. Surrounding hydrophobic residues, including Asp325, Glu327, Thr114, Ala115, Ala116, Ala117, and Cys326, further compact the binding pocket, contributing to the ligand's proper positioning, as illustrated in Fig. 4b and detailed in Table 2.

The aurintricarboxylic acid with HMPV(5WB0) complex

The aurintricarboxylic acid *with HMPV(5WB0)* complex interacts with several residues through both hydrogen bonding and hydrophobic interactions. Key hydrogen bonds are observed with Thr114(A), Ala115(A), Ala109(A), and Arg101(A), with bond distances ranging from 2.61 Å to 3.05 Å. In addition, hydrophobic contacts are formed with residues such as Ala338, Ala339, Asp325, Ala116, Val112, Ile108, Leu110, and Pro98. These interactions suggest that the ligand is stabilized mainly by a combination of backbone hydrogen bonds and a supportive hydrophobic environment, as illustrated in Fig. 4c and detailed in Table 2.

Molecular dynamics analysis

The RMSD of HMPV protein model with salvianolic acid C provides insights into the structural stability and deviation from the initial conformation over time. The Mycophenolic acid (red trajectory) shows significant fluctuations, reaching values above 10 nm, which reflects very high conformational flexibility. On the other hand, the Salvianolic acid C (black) and Aurintricarboxylic acid (green) trajectories remain below 1 nm with minimal fluctuations throughout the 100 ns simulation. This suggests that these two systems maintain high structural stability and are less prone to large conformational changes, highlighting their stable dynamic behavior compared to the Mycophenolic acid system complex as shown in Fig. 5a.

The RMSF graph Fig. 5b evaluates the flexibility of individual residues/atoms. All three systems Ligands (Black - Salvianolic acid C, Red - Mycophenolic acid, Green - Aurintricarboxylic acid) follow a similar pattern of fluctuations, with peaks observed in specific regions, likely corresponding to loop or terminal regions that are generally more flexible. The fluctuation amplitude remains below 0.5 nm for most residues, except for certain peaks around atom indices ~ 2000, ~4000, and ~ 6500, where enhanced flexibility is observed. This indicates that the overall backbone stability is retained, while only specific regions contribute to local fluctuations. Notably, there are no extreme spikes suggesting severe instability in any of the systems.

The radius of gyration is a property of the protein-ligand complex axis of rotation. As shown in Fig. 5c, The radius of gyration plot shows the compactness of the system over the simulation time (100 ns). The Mycophenolic acid remains relatively stable around 3.1–3.2 nm, suggesting that this structure maintains its overall compactness and does not undergo major conformational collapse. In contrast, the Aurintricarboxylic acid and Salvianolic acid C trajectories show a gradual decrease in Rg values, stabilizing closer to 2.9–3.0 nm. This indicates that these systems undergo compaction during the simulation, suggesting a more stable and tighter packing of the structure compared to the Mycophenolic acid system.

The H-bond analysis revealed that the HMPV protein model with salvianolic acid C complex maintains one H-bond continuously throughout the MD simulation, as shown in Fig. 6a. Whereas the HMPV protein model with Mycophenolic acid and HMPV protein model with Aurintricarboxylic Acid complexes did not maintain hydrogen bonds continuously throughout the MD simulation, as shown in Fig. 6b,c.

The HMPV protein model with salvianolic acid C complex in Fig. 6a exhibited a maximum of four H-bonds and an average of one H-bond throughout the simulation, with a 20.97% H-bond occupancy between GLU96 of the HMPV complex and the salvianolic acid ligand (Table 3) indicating good stability in the HMPV protein model with salvianolic acid C complex. For the HMPV protein model with mycophenolic acid complex in Fig. 6b, an average of zero H-bonds was observed throughout the simulation, with the highest bond occupancy of 0.08% (Table 3) occurring between ARG91 of the HMPV protein model and the mycophenolic acid ligand. In the HMPV protein model with Aurintricarboxylic Acid complex in Fig. 6c, exhibited a maximum of three H-bonds and an average of one H-bond throughout the simulation, with the highest bond occupancy of 84.97% (Table 3) occurring between ASP325 of the HMPV complex and the Aurintricarboxylic Acid ligand, indicating an stable complex as H-bonds were maintained throughout the MD simulation.

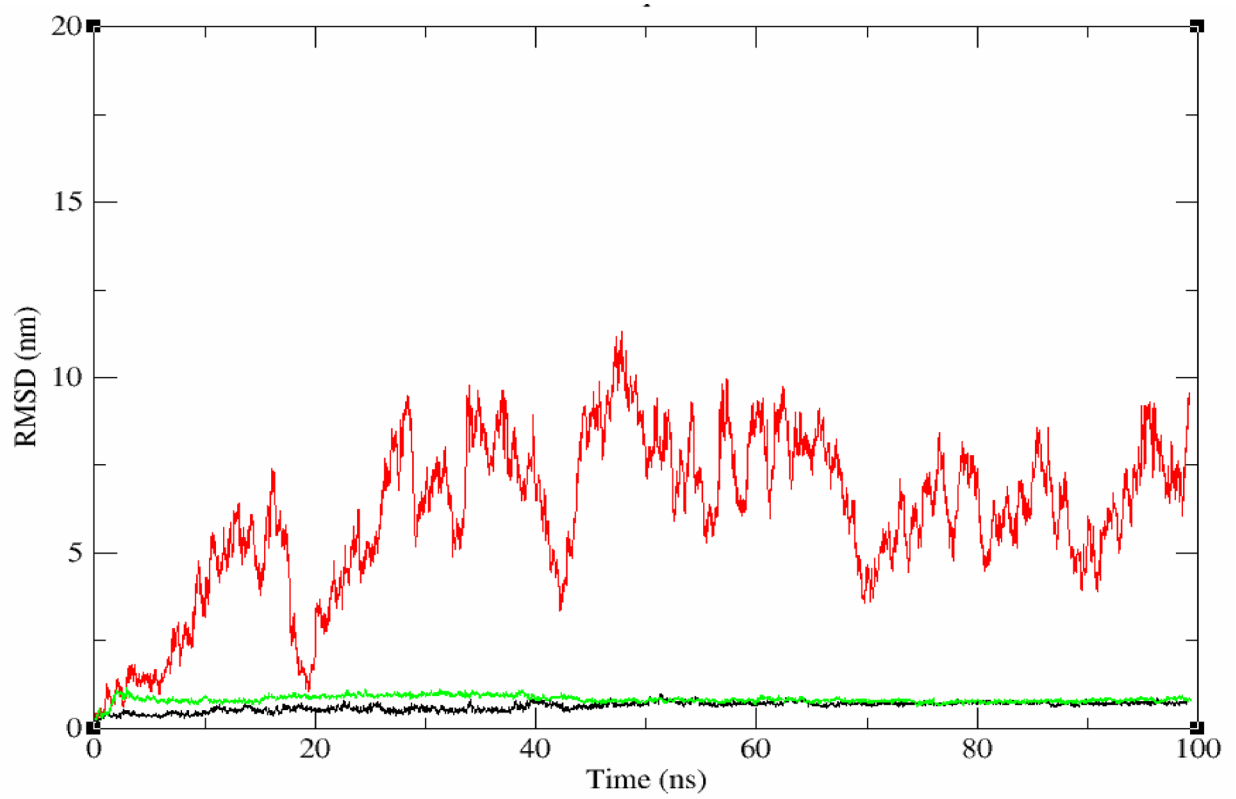

(a)

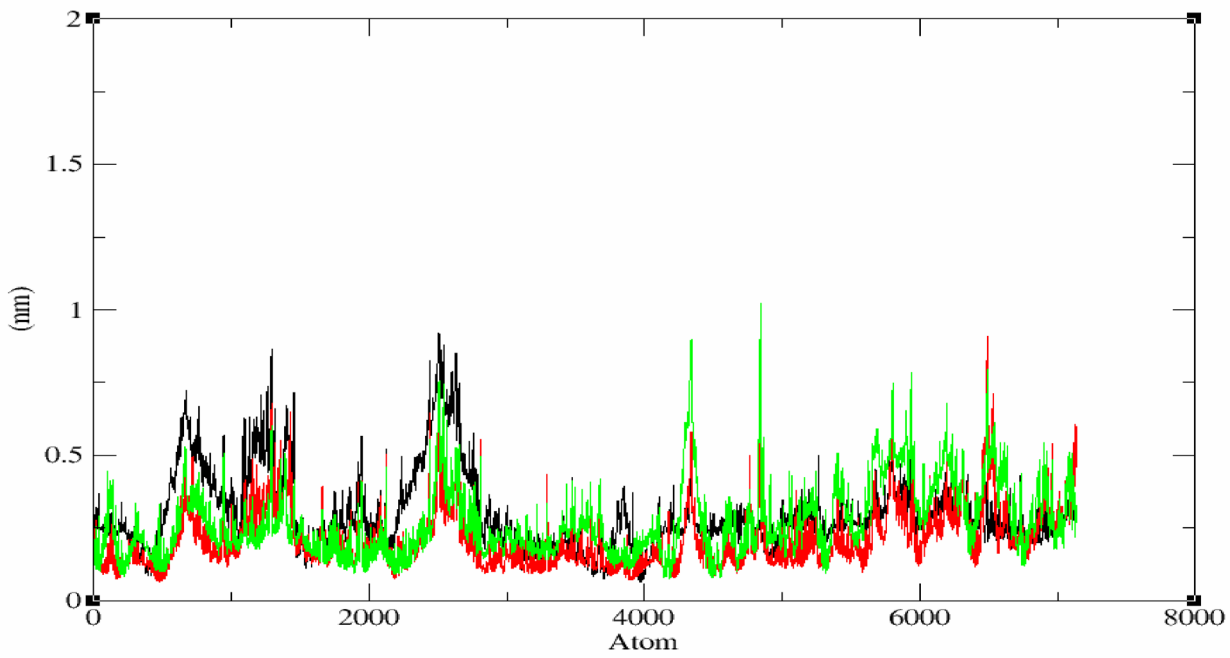

(b)

Fig. 5. (**a**) RMSD of HMPV(5WB0) complex with ligands (Black - Salvianolic acid C, Red - Mycophenolic acid, Green - Aurintricarboxylic acid); (**b**) RMSF of HMPV(5WB0) complex with Ligands (Black - Salvianolic acid C, Red - Mycophenolic acid, Green - Aurintricarboxylic acid); and (**c**) Radius of Gyration of HMPV(5WB0) complex with Ligands (Black - Salvianolic acid C, Red - Mycophenolic acid, Green - Aurintricarboxylic acid).

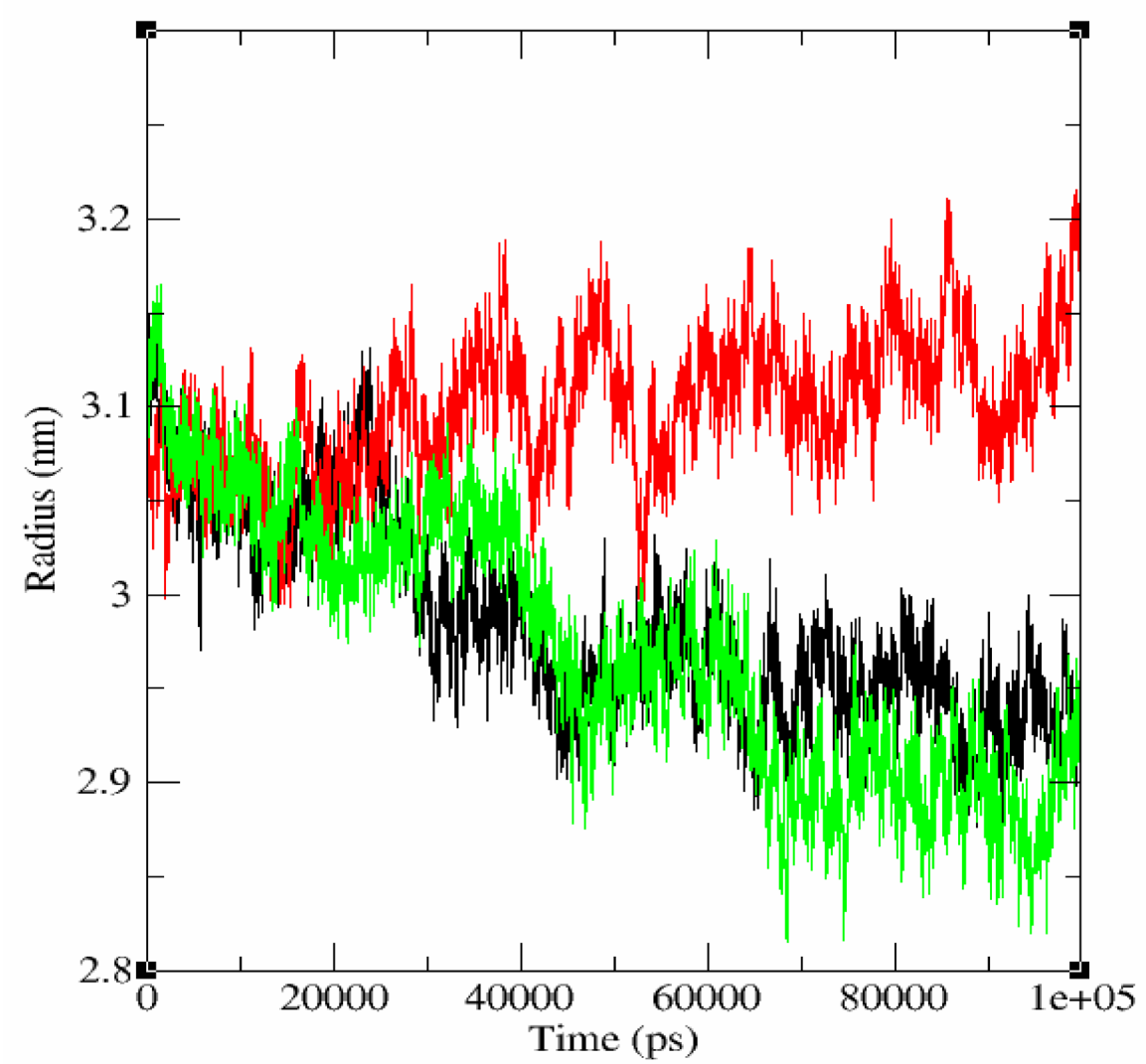

(c)

Fig. 5. (continued)

Binding free energy calculation analysis

The overall end-state binding free energy is −26.12 kcal/mol for the HMPV-Salvianolic Acid C complex (Fig. 7a), −0.54 kcal/mol for the HMPV-Mycophenolic Acid complex (Fig. 7b), and −25.29 kcal/mol for the HMPV-Aurintricarboxylic Acid complex (Fig. 7c). Thus, it is evident that the complex, HMPV protein with salvianolic acid C, has higher negative binding free energy, making it the best drug candidate against the HMPV protein complex.

PCA and FEL analysis

To further analyze the distribution of the structural conformations from the MD simulation trajectories, the PC1 and PC2 were mapped on 2D space and 3D space to understand the conformational changes by determining the low-energy basins (minima). The results of a free energy landscape after 100 ns are shown in Fig. 8a,c,e for 2D images) and Fig. 8b,d,f for 3D images). The dark blue spots with a red point indicate the energy minima and energetically favored protein conformations, and the yellow spots reflect the unfavorable conformations in Fig. 8. The shallow and narrow energy basin observed during the simulation revealed the low stability of the protein-ligand complex.

Figure 8a,b shows two well-defined low-energy basins, suggesting stable conformations. In contrast, Fig. 8c–f display fragmented low-energy regions with higher maximum free energy values (9.67 and 12.5 kJ/mol, respectively), indicating increased conformational heterogeneity and potentially weaker or unstable binding. Thus, Fig. 8a,b HMPV protein model with salvianolic acid C complex exhibits a stable binding mode with well-defined, deep free energy basins.

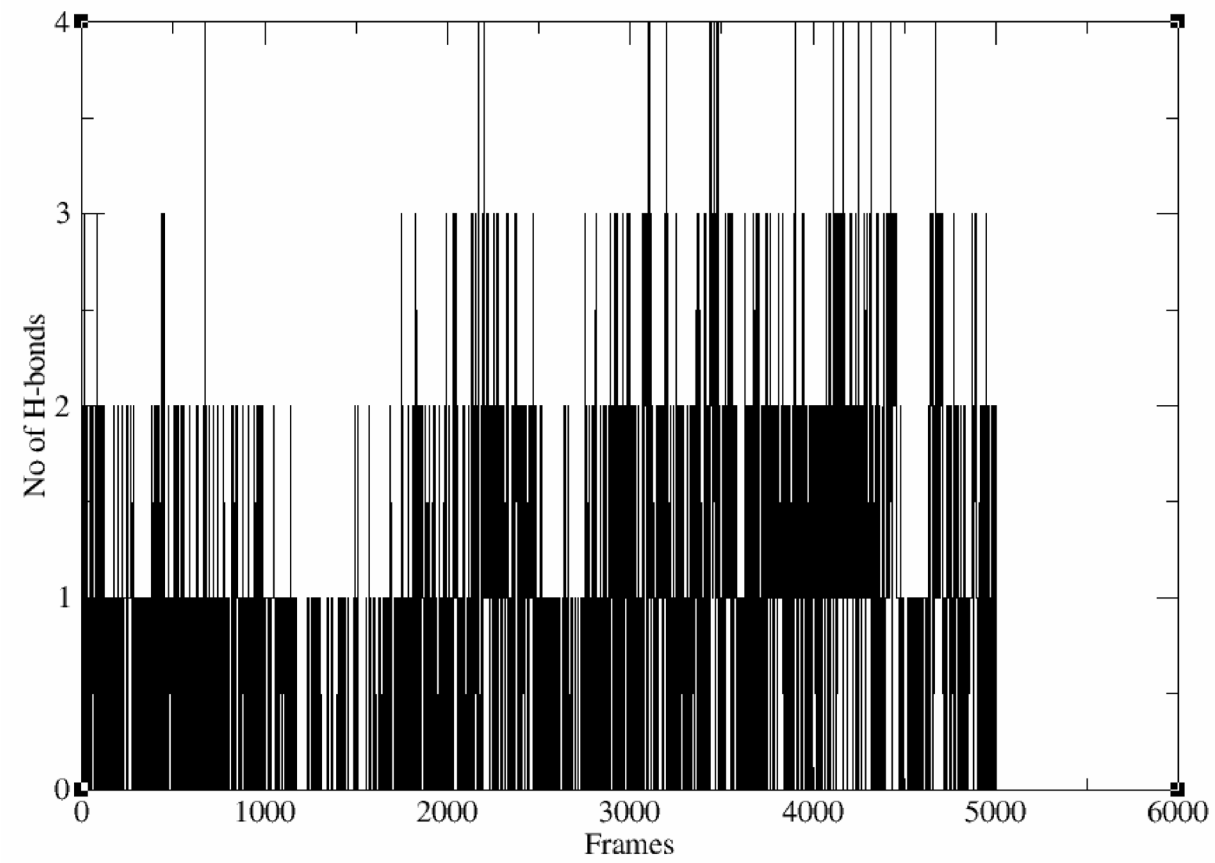

(a)

Fig. 6. Number of H-bonds of HMPV(5WB0) complex with ligands (**a**) salvianolic acid C, (**b**) mycophenolic acid, and (**c**) aurintricarboxylic acid.

Discussion

The findings of this study highlight the potential of repurposing SARS-CoV-2 ligands for therapeutic intervention against Human Metapneumovirus (HMPV), a significant respiratory pathogen with no currently approved antiviral treatments or vaccines. Through a comprehensive computational approach, we evaluated the binding affinity, stability, and interaction dynamics of three ligands Salvianolic Acid C, Mycophenolic Acid, and Aurintricarboxylic Acid with the HMPV protein structure. Comparing the molecular docking results, the ligand is consistently stabilized by an alanine-rich hydrophobic pocket, but the degree of interaction varies. In Aurintricarboxylic Acid, stabilization relies mainly on a few key hydrogen bonds and hydrophobic support. In Mycophenolic Acid, charged residues like Lys324 and Arg91 provide electrostatic contributions that enhance binding. Salvianolic Acid C, however, shows the most extensive binding network, involving multiple hydrogen bonds with both charged and polar residues, supported by many hydrophobic contacts, suggesting that it represents the strongest binding mode of the ligand. The results provide valuable insights into the potential of these compounds as anti-HMPV agents, with Salvianolic Acid C emerging as the most promising candidate.

Stability and binding affinity of ligand-HMPV complexes

The molecular dynamics (MD) simulations revealed distinct stability profiles for the three ligand-HMPV complexes. The HMPV-Salvianolic Acid C complex demonstrated the most stable binding, as evidenced by its consistent RMSD values (5–6 Å) throughout the 100 ns simulation. In contrast, the HMPV-Mycophenolic Acid complex exhibited significant fluctuations. The HMPV-Aurintricarboxylic Acid complex displayed the stability, with RMSD values (8–9 Å) throughout the 100 ns simulation. These observations were further supported by the Root Mean Square Fluctuation (RMSF) analysis, which showed minimal residual fluctuations for the Salvianolic Acid C complex, compared to increased fluctuations in the Mycophenolic Acid and Aurintricarboxylic Acid complexes.

Hydrogen bond analysis provided additional evidence for the stability of the HMPV-Salvianolic Acid C complex. The complex maintained an average of one hydrogen bond throughout the simulation, with a 20.97% H-bond occupancy between GLU96 of HMPV protein model and Salvianolic Acid C. In contrast, the other two ligands exhibited lower hydrogen bond occupancy and failed to maintain consistent interactions, further underscoring the superior binding stability of Salvianolic Acid C.

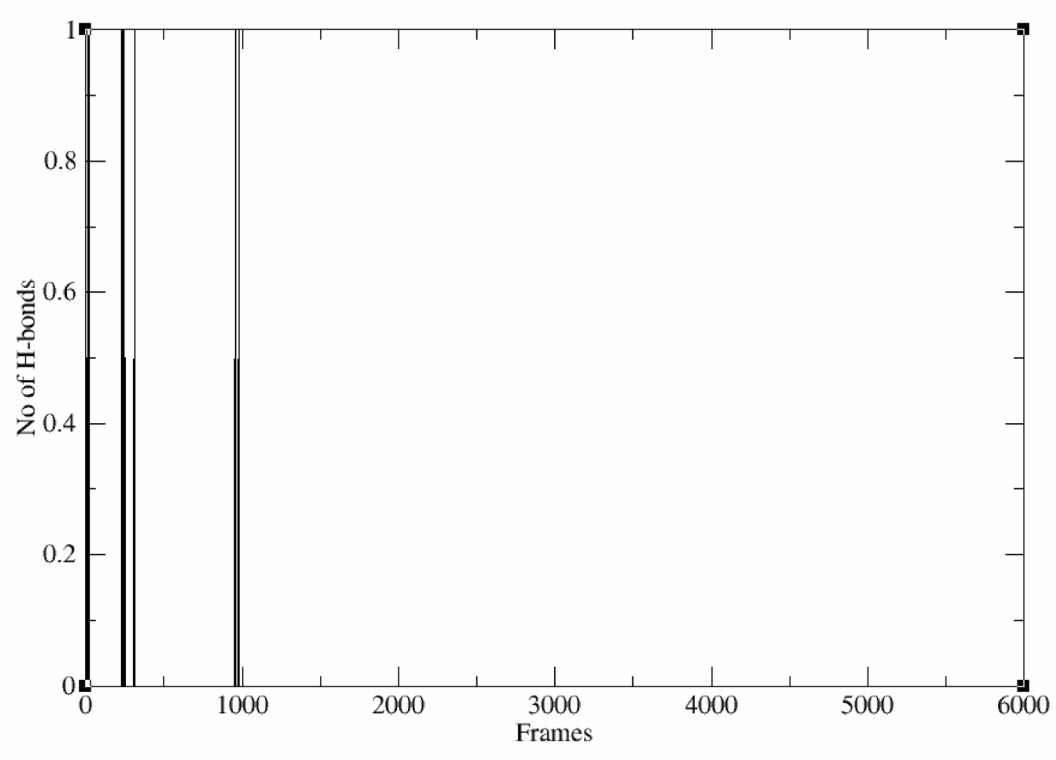

(b)

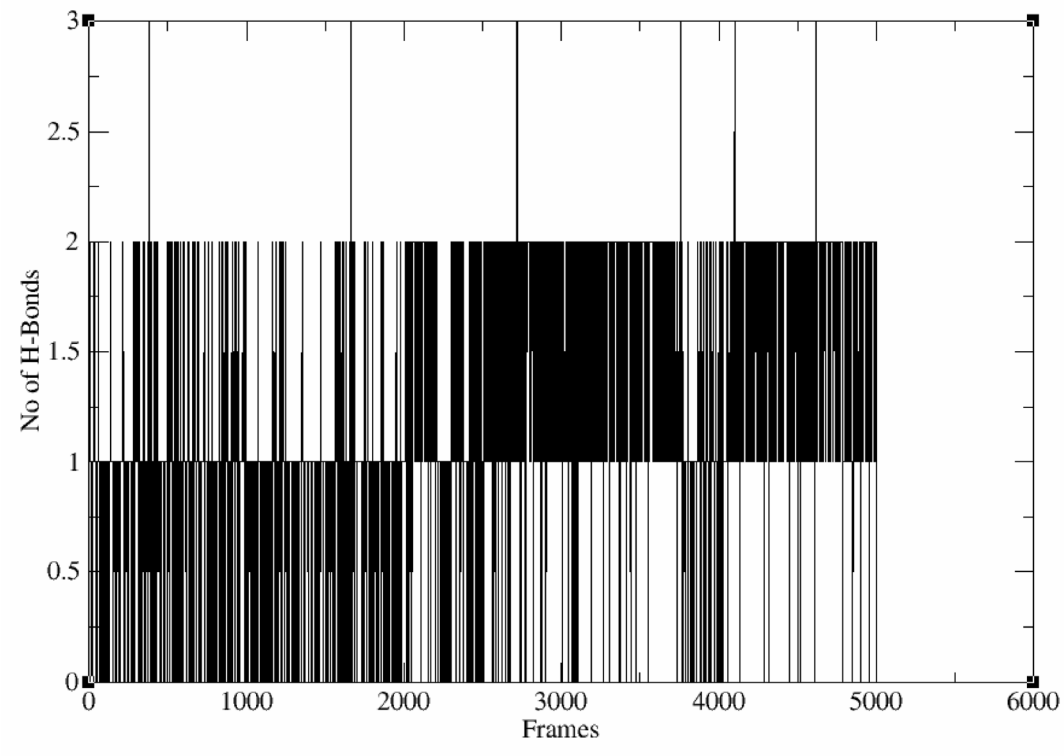

(c)

Fig. 6. (continued)

Binding free energy and thermodynamic stability

The binding free energy calculations corroborated the MD simulation results, with the HMPV-Salvianolic Acid C complex exhibiting the most favorable binding free energy (−26.11 kcal/mol). This value was significantly lower than those of the HMPV-Mycophenolic Acid (−0.54 kcal/mol) and HMPV-Aurintricarboxylic Acid

H-bonds occupancy			
Complex	**HMPV**	**Ligand**	**Occupancy %**
HMPV (5WB0) complex with Salvianolic Acid C (SAC)	GLU96	SAC	20.97
	GLU327	SAC	19.57
	GLU96	SAC	10.38
	ASP325	SAC	9.86
HMPV (5WB0) complex with Mycophenolic Acid (MPA)	ARG91	MPA	0.08
	LEU89	MPA	0.08
HMPV (5WB0) complex with Aurintricarboxylic Acid (ATA)	ASP325	ATA	84.97
	SER482	ATA	38.76

Table 3. H-bond occupancy of HMPV (5WB0) complex with ligands salvianolic acid C, mycophenolic acid, and aurintricarboxylic acid.

(−25.29 kcal/mol) complexes, indicating stronger thermodynamic stability and a higher likelihood of effective binding. The negative binding free energy of Salvianolic Acid C suggests that it forms a stable and energetically favorable complex with HMPV protein model, making it a promising candidate for further development.

Conformational dynamics and free energy landscape

Principal Component Analysis (PCA) and Free Energy Landscape (FEL) analysis provided further insights into the conformational dynamics of the ligand-HMPV complexes. The HMPV-Salvianolic Acid C complex exhibited well-defined, deep free energy basins, indicative of stable and energetically favored conformations. In contrast, the HMPV-Mycophenolic Acid and HMPV-Aurintricarboxylic Acid complexes displayed fragmented low-energy regions with higher maximum free energy values, reflecting increased conformational heterogeneity and weaker binding. These findings align with the RMSD and RMSF results, reinforcing the conclusion that Salvianolic Acid C forms the most stable and specific interactions with the HMPV protein model used in this study.

Implications for drug development

The results of this study underscore the potential of Salvianolic Acid C as a lead compound for anti-HMPV therapy. Its potent antioxidant and anti-inflammatory properties, combined with its stable binding to HMPV protein model, make it a promising candidate for further experimental validation. While Mycophenolic Acid and Aurintricarboxylic Acid also demonstrated some inhibitory potential, their lower binding stability and higher conformational heterogeneity limit their therapeutic prospects. However, these compounds could serve as starting points for structural optimization to improve their binding affinity and stability.

Limitations and future directions

While the computational approach employed in this study provides valuable insights, it is important to acknowledge its limitations. The simulations were conducted in silico, and experimental validation is necessary to confirm the binding affinity and antiviral efficacy of the identified ligands. Additionally, the study focused on a single HMPV protein structure (PDB ID: 5WB0), and future work should explore the interactions of these ligands with other HMPV protein model subtypes and protein conformations. Furthermore, the pharmacokinetic and pharmacodynamic properties of Salvianolic Acid C, including its bioavailability and toxicity, need to be evaluated in preclinical studies.

Conclusion

In conclusion, this study employed a comprehensive computational approach to evaluate the potential of repurposing SARS-CoV-2 ligands such as Salvianolic Acid C, Mycophenolic Acid, and Aurintricarboxylic Acid as therapeutic agents against Human Metapneumovirus (HMPV) protein model. Molecular docking, MD simulations, binding free energy calculations, and PCA collectively demonstrated that Salvianolic Acid C exhibits the strongest binding affinity and stability with HMPV protein model, supported by consistent RMSD values, low residual fluctuations, and a favorable binding free energy of −26.12 kcal/mol. Additionally, hydrogen bond analysis revealed a stable interaction with GLU96, further reinforcing its potential as an effective antiviral candidate. In contrast, Mycophenolic Acid and Aurintricarboxylic Acid displayed weaker binding and higher conformational instability. These findings position Salvianolic Acid C as a promising lead compound for anti-HMPV therapy, addressing the urgent need for effective treatments against this widespread respiratory pathogen. However, further in vitro and in vivo studies are essential to validate its efficacy and safety. This study lays a crucial foundation for future research into repurposed antiviral therapies, offering a potential pathway toward combating infections in the absence of approved vaccines or antivirals.

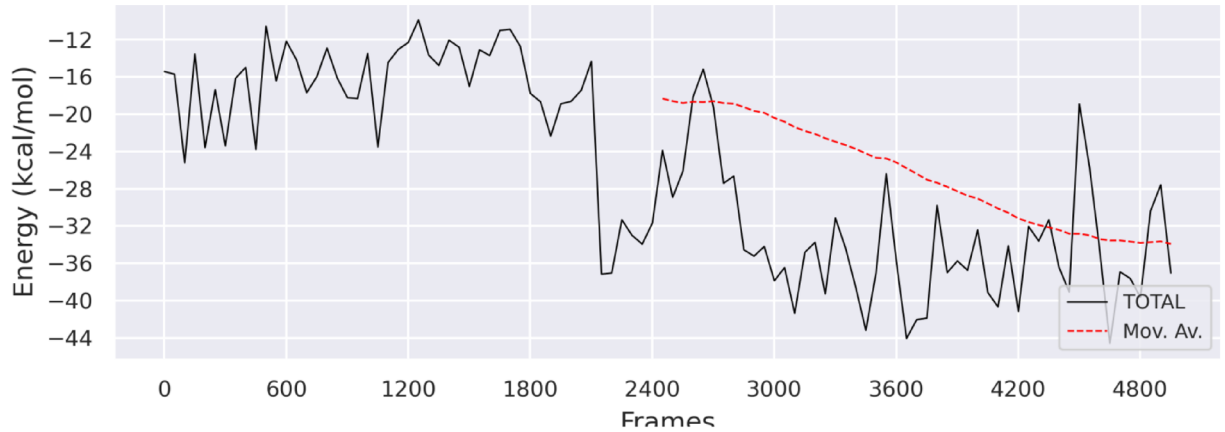

(a)

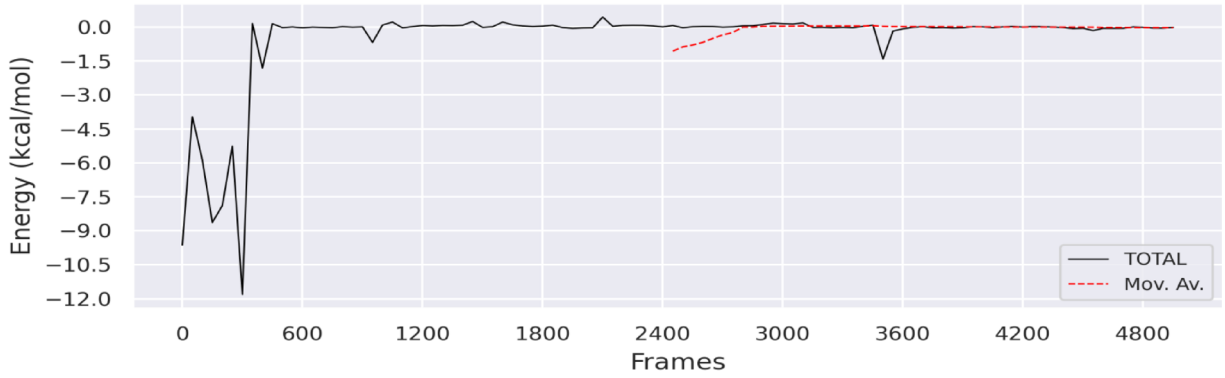

(b)

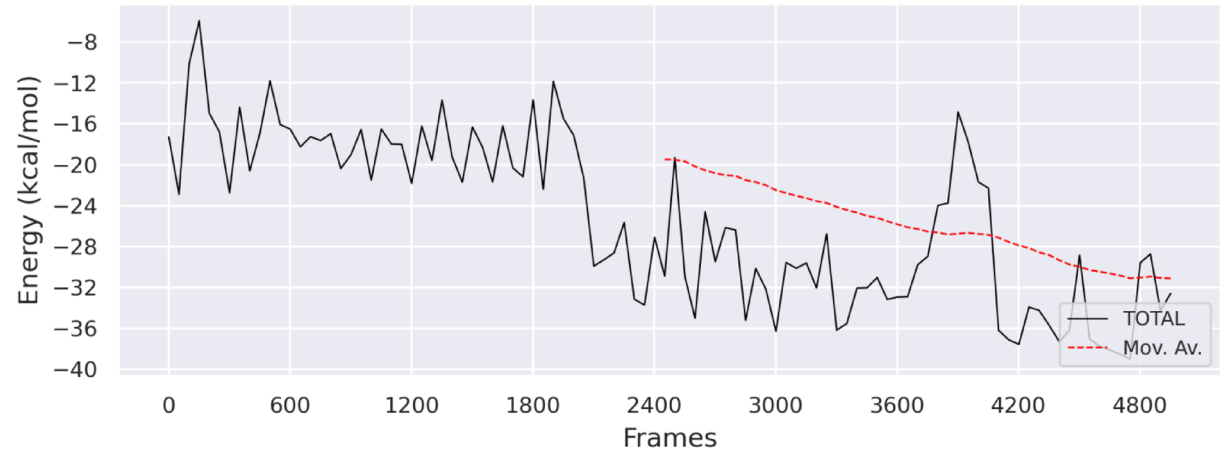

(c)

Fig. 7. Binding free energy of HMPV(5WB0) complex with ligands (**a**) Salvianolic acid C, (**b**) Mycophenolic acid, and (**c**) Aurintricarboxylic acid.

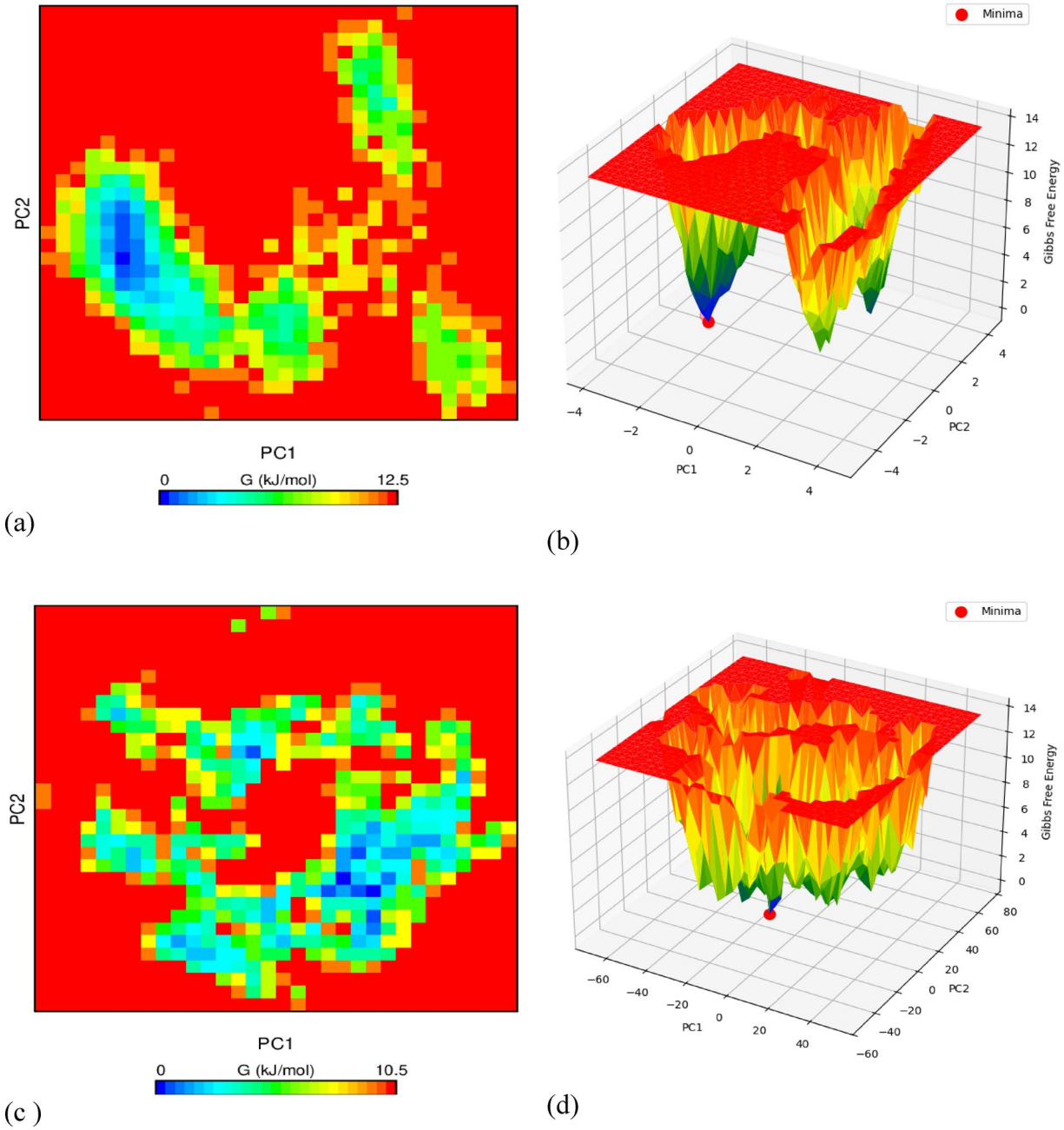

Fig. 8. Free Energy Landscape Minima 2D Plot of HMPV(5WB0) Complex with Ligands (**a**) salvianolic acid C, (**c**) mycophenolic acid, and (**e**) aurintricarboxylic acid. Free Energy Landscape Minima 3D Plot of HMPV(5WB0) Complex with Ligands (**b**) salvianolic acid C, (**d**) mycophenolic acid, and (**f**) aurintricarboxylic acid.

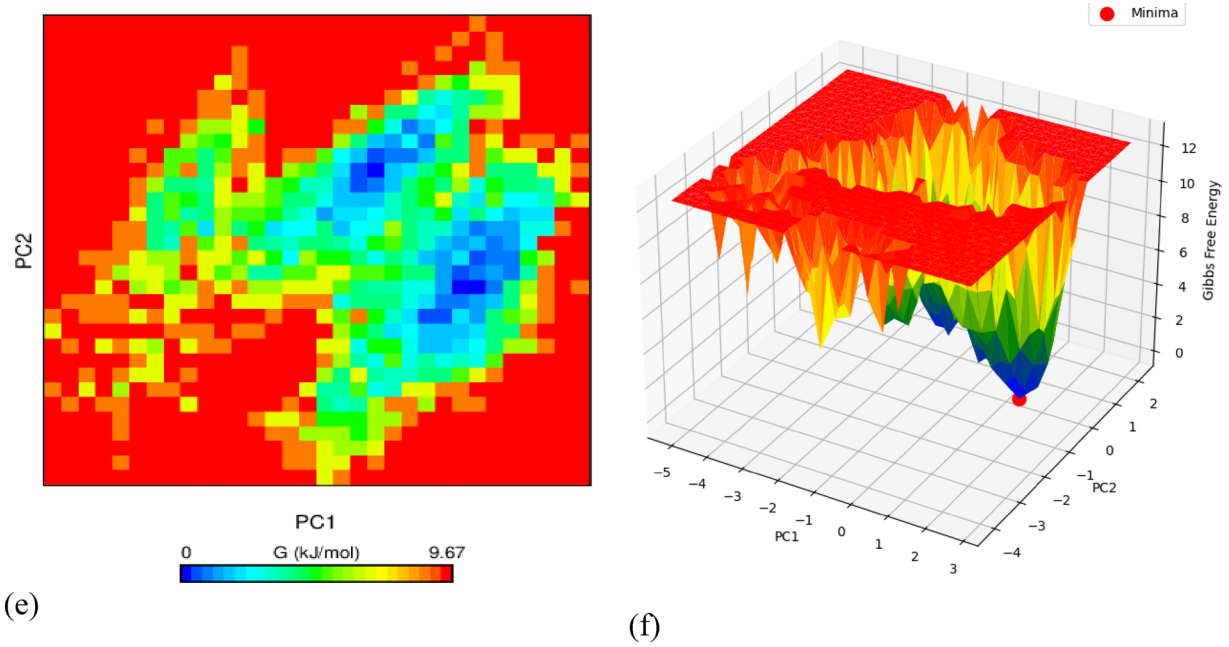

Fig. 8. (continued)

Data availability

The datasets generated and/or analysed during the current study are available in the Mendeley Data repository, [https://data.mendeley.com/datasets/23dp444hgw/1] (https:/data.mendeley.com/datasets/23dp444hgw/1).

Received: 23 April 2025; Accepted: 6 November 2025
Published online: 10 December 2025

References

1. Williams, J. V. et al. Human metapneumovirus infection in children hospitalized for wheezing. *J. Allergy Clin. Immunol.* **115** (6), 1311. https://doi.org/10.1016/j.jaci.2005.02.001 (2005).
2. Shafagati, N. & Williams, J. V. Human metapneumovirus - what we know now. *F1000Research* https://doi.org/10.12688/f1000research.12625.1 (2018).
3. Akingbola, A. et al. Human Metapneumovirus: an emerging respiratory pathogen and the urgent need for improved Diagnostics, surveillance, and vaccine development. *Infect. Dis.* https://doi.org/10.1080/23744235.2025.2453824 (2025).
4. Schildgen, O., Simon, A. & Williams, J. V. NaN. Animal models for human metapneumovirus (HMPV) infections. *Vet. Res.* https://doi.org/10.1051/VETRES:2006051 (2007).
5. Boggs, K. et al. Human metapneumovirus phosphoprotein independently drives phase separation and recruits nucleoprotein to Liquid-Like bodies. *mBio* https://doi.org/10.1128/mbio.01099-22 (2022).
6. Nao, N. et al. Recent molecular evolution of human metapneumovirus (HMPV): subdivision of HMPV A2b strains. *Microorganisms* https://doi.org/10.3390/microorganisms8091280 (2020).
7. Du, Y., Li, Wei, Guo, Yajun, Li, Lin, Chen, Q., He, L. & Shang, S. Epidemiology and genetic characterization of human metapneumovirus in pediatric patients from Hangzhou China. *J. Med. Virol.* https://doi.org/10.1002/jmv.28024 (2022).
8. Shirato, K. et al. Molecular epidemiology of human metapneumovirus before and after COVID-19 in East Japan in 2017–2022. *None* https://doi.org/10.7883/yoken.JJID.2023.350 (2023).
9. Alto, W. A. Human metapneumovirus: a newly described respiratory tract pathogen. *J. Am. Board. Family Pract.* **17** (6), 466–469. https://doi.org/10.3122/jabfm.17.6.466 (2004).
10. Más, V. et al. Engineering, structure and immunogenicity of the human metapneumovirus F protein in the postfusion conformation. *PLoS pathog.* **12**(9), e1005859. https://doi.org/10.1371/journal.ppat.1005859 (2016).
11. Rib-Molina, P. et al. Human metapneumovirus infection of organoid-derived human bronchial epithelium represents cell tropism and cytopathology as observed in in vivo models. *Msphere* https://doi.org/10.1128/msphere.00743-23 (2024).
12. Chang, A., Masante, C., Buchholz, U. & Dutch, R. Human metapneumovirus (HMPV) binding and infection are mediated by interactions between the HMPV fusion protein and Heparan sulfate. *J. Virol.* https://doi.org/10.1128/JVI.06706-11 (2012).
13. Ballegeer, M. et al. A neutralizing single-domain antibody that targets the trimer interface of the human metapneumovirus fusion protein. *mBio* https://doi.org/10.1128/mbio.02122-23 (2023).
14. Najjar, F. E. et al. Imaging analysis reveals budding of filamentous human metapneumovirus virions and direct transfer of inclusion bodies through intercellular extensions. *mBio* https://doi.org/10.1128/mbio.01589-23 (2023).
15. Bergh, A., Van Den, Guillon, Patrice, Itzstein, M., Von, Bailly, B. & Dirr, L. *Drug Repurposing for Therapeutic Discovery against Human Metapneumovirus Infection*. bioRxiv. https://doi.org/10.1128/aac.01008-22 (2022).
16. Sumitomo, K. et al. Human metapneumovirus-associated community-acquired pneumonia in adults during the first wave of COVID-19. *J. Rural Med.* https://doi.org/10.2185/jrm.2021-035 (2021).
17. Kitanovski, L. et al. Treatment of severe human metapneumovirus (hMPV) pneumonia in an immunocompromised child with oral ribavirin and IVIG. *J. Pediatr. Hematol. Oncol.* https://doi.org/10.1097/MPH.0b013e3182915d2d (2013).
18. Shehu, M., Pascual, A. & Khoury, Marc, Y. E. Mortality and Morbidity of Human Metapneumovirus Infection in the Pre-COVID-19 Era: The Value of the Charlson Comorbidity Index on Outcome Prediction. *Cureus* https://doi.org/10.7759/cureus.52321 (2024).

19. Yang, C. et al. Salvianolic acid C potently inhibits SARS-CoV-2 infection by blocking the formation of six-helix bundle core of Spike protein. *Sig Transduct. Target. Ther.* **5**, 220. https://doi.org/10.1038/s41392-020-00325-1 (2020).
20. Ma, L. & Tang, L. Salvianolic acids: potential source of natural drugs for the treatment of fibrosis disease and cancer. *Front. Pharmacol.* **10**, 97. https://doi.org/10.3389/fphar.2019.00097 (2019).
21. Benjanuwattra, J., Chaiyawat, P., Pruksakorn, D. & Koonrungsesomboon, N. Therapeutic potential and molecular mechanisms of mycophenolic acid as an anticancer agent. *Eur. J. Pharmacol.* **887**, 173580. https://doi.org/10.1016/j.ejphar.2020.173580 (2020).
22. Stewart, M. L., Grollman, A. P. & Huang, M. T. Aurintricarboxylic acid: inhibitor of initiation of protein synthesis. *Proc. Natl. Acad. Sci. U S A*. **68** (1), 97–101. https://doi.org/10.1073/pnas.68.1.97 (1971). PMID: 5276307; PMCID: PMC391170.
23. Kim, S. et al. Pubchem in 2021: new data content and improved web interfaces. *Nucleic Acids Res.* **49**(D1), D1388–D1395. https://doi.org/10.1093/nar/gkaa971 (2021).
24. Noel, M., O'Boyle, M., Banck, C. A. & James Chris Morley, TimVandermeersch, and Geoffrey R Hutchison. Open babel: an open chemical toolbox. *J. Cheminform.* **3** (1), 1–14 (2011). https://www.cheminfo.org/Chemistry/Cheminformatics/FormatConverter/index.html
25. Eric, F. et al. Meng, and Thomas E Ferrin.Ucsf chimera—a visualization system for exploratory research and analysis. *J. Comput. Chem.* **25**(13), 1605–1612 (2004).
26. Neese, F., Wennmohs, F., Riplinger, C. & Ute Becker, and The ORCA quantum chemistry program package. *J. Chem. Phys.* **152**, 22 (2020).
27. Hanwell, M. D. et al. Hutchison. Avogadro: an advanced semantic chemical editor, visualization, and analysis platform. *J. Cheminform.* **4** (1), 17 (2012).
28. Abkari, A., Chaabane, I. & Guidara, K. DFT (B3LYP/LanL2DZ and B3LYP/6311G+ (d, p)) comparative vibrational spectroscopic analysis of organic–inorganic compound Bis (4-acetylanilinium) tetrachlorocuprate (II). *Phys. E.* **81**, 136–144 (2016).
29. Rovira, C. Study of ligand-protein interactions by means of density functional theory and first-principles molecular dynamics. In *Protein-Ligand Interactions: Methods and Applications* 517–553 (Humana, 2005).
30. De Jesús-González, L. et al. Advances and challenges in antiviral development for respiratory viruses. *Pathogens* **14**(1), 20 (2024).
31. Tian, W., Chen, C., Lei, X., Zhao, J. & Liang, J. Castp3.0: computed atlas of surface topography of proteins.Nucleic acids research. *Nucleic Acids Res.* **46**(W1), W363–W367. https://doi.org/10.1093/nar/gky473 (2018).
32. Honorato, R. V. et al. The HADDOCK2.4 web server for integrative modeling of biomolecular complexes. *Nat. Protoc.* **19**, 3219–3241. https://doi.org/10.1038/s41596-024-01011-0 (2024).
33. Laskowski, R. A., Mark, B. & Swindells,. LigPlot+: multiple ligand–protein interaction diagrams for drug discovery. *J. Chem. Inf. Model* **51**, 2778–2786 (2011).
34. Pronk, S. et al. Gromacs 4.5: a high-throughput and highly parallel open source molecular simulation toolkit. *Bioinformatics* **29** (7), 845–854 (2013).
35. Piana, K. L. L. S. et al. Improved side-chaintorsion potentials for the amber ff99sb protein force field. *Proteins: Struct. Funct. Bioinformat.* **78**(8), 1950–1958. https://doi.org/10.1002/prot.22711 (2010).
36. David, A. et al. The amber biomolecular simulationprograms. *J. comput. chem.* **26**(16), 1668–1688 (2005).
37. Gotz, R. S. F. A. W. & Poole, D. ScottLe Grand, and Ross C Walker. Routine microsecond molecular dynamics simulations with amber on gpus. 2. explicit solvent particle mesh Ewald. *J. Chem. Theory Comput.* **9** (9), 3878–3888 (2013).
38. Yujie Wu, Harald, L., Tepper, Gregory, A. & Voth Flexible simplepoint-charge water model with improved liquid-state properties. *TheJournal Chem. Phys.* **124** (2), 024503 (2006).
39. PJ Turner. *Xmgrace, Center for Coastal and Land-Margin Research*. version 5.1. 19 (Oregon Graduate Institute of Science and Technology, 2005).
40. Miller, I. I. I. et al. MMPBSA. Py: an efficient program for end-state free energy calculations. *J. Chem. Theory Comput.* **8** (9), 3314–3321 (2012).
41. Maisuradze, G. G. Leitner. Free energy landscape of a biomolecule in dihedral principal component space: sampling convergence and correspondence between structures and minima. *Proteins Struct. Funct. Bioinform.* **67** (3), 569–578 (2007).
42. Mitra, D., Afreen, S., Das Mohapatra, P. K. & Abdalla, M. Inhibition of respiratory syncytial virus by Daclatasvir and its derivatives: synthesis of computational derivatives as a new drug development. *J. Biomol. Struct. Dynamics*. **43** (5), 2440–2462 (2025).
43. Mitra, D. et al. Potentiality of bioactive compounds as inhibitor of M protein and F protein function of human respiratory syncytial virus. *Silico Pharmacol.* **12**, 5. https://doi.org/10.1007/s40203-023-00178-w (2024).
44. Mitra, D., Paul, M., Thatoi, H. & Mohapatra, P. K. D. Study of potentiality of dexamethasone and its derivatives against Covid-19. *J. Biomol. Struct. Dynamics*. **40** (20), 10239–10249. https://doi.org/10.1080/07391102.2021.1942210 (2021).
45. Biswas, I. & Debanjan Mitra Comparative analysis of RuBisCO evolution and intrinsic differences: insights from in Silico assessment in Cyanobacteria, Monocot, and Dicot plants. *Biology Life Sci. Forum*. **27** (1), 44. https://doi.org/10.3390/IECAG2023-15820 (2023).
46. Biswas, I. Insilico sequence-structure based analysis of bacterial chromate reductase to unravel enzymatic specificity towards chromium pollution. *Biocatal. Agric. Biotechnol.* **60**, 103339 (2024).
47. Biswas, I. et al. Enhanced antibacterial effect of natural tannin stabilized silver nano particles against human pathogens: a target toward FtsZ proteins. *J. Trace Elem. Minerals*. **10**, 100200 (2024).

Author contributions

P.M.S wrote the main manuscript text. N.M and S.P.K reviewed the manuscript.

Declarations

Competing interests

The authors declare no competing interests.

Additional information

Correspondence and requests for materials should be addressed to P.M.S.

Reprints and permissions information is available at www.nature.com/reprints.

Publisher's note Springer Nature remains neutral with regard to jurisdictional claims in published maps and institutional affiliations.